

See discussions, stats, and author profiles for this publication at: <https://www.researchgate.net/publication/231730570>

# Intermetallic Bonds in Metallophilic Mercuriaazametallamacrocycles of Synthetic Design

ARTICLE *in* ORGANOMETALLICS · SEPTEMBER 2010

Impact Factor: 4.13 · DOI: 10.1021/om100297v

---

CITATIONS

13

---

READS

32

7 AUTHORS, INCLUDING:



**Sagar Sharma**

Weizmann Institute of Science

24 PUBLICATIONS 181 CITATIONS

SEE PROFILE



**Sandip Dey**

Bhabha Atomic Research Centre

44 PUBLICATIONS 542 CITATIONS

SEE PROFILE



**Ray J. Butcher**

Howard University

1,042 PUBLICATIONS 9,370 CITATIONS

SEE PROFILE

## Intermetallic Bonds in Metallophilic Mercuraazametallamacrocycles of Synthetic Design

Upali Patel,<sup>†</sup> Sagar Sharma,<sup>†</sup> Harkesh B. Singh,<sup>\*,†</sup> Sandip Dey,<sup>‡</sup> Vimal K. Jain,<sup>‡</sup>  
Gotthelf Wolmershäuser,<sup>§</sup> and Ray J. Butcher<sup>||</sup><sup>†</sup>Department of Chemistry, Indian Institute of Technology Bombay, Mumbai 400076, India,<sup>‡</sup>Chemistry Division, Bhabha Atomic Research Centre, Mumbai 400085, India, <sup>§</sup>Fachbereich Chemie, Universität Kaiserslautern, Postfach 3049, Kaiserslautern 67653, Germany, and <sup>||</sup>Department of Chemistry, Howard University, Washington, D.C. 20059

Received April 13, 2010

22-Membered mercuraazametallamacrocycles **6**, **7**, and **12** have been synthesized by dipodal condensation (2 + 2) of bis(*o*-formylphenyl)mercury (**11**) and 1,2-disubstituted amines. Reduction of macrocycle **6** with sodium borohydride afforded novel 11-membered mercuraazametallamacrocycle **13**. Macrocycle **6**, when treated with [Cu(CH<sub>3</sub>CN)<sub>4</sub>]ClO<sub>4</sub> and Cu(OCOCH<sub>3</sub>)<sub>2</sub>/NH<sub>4</sub>PF<sub>6</sub>, formed orange-colored Cu<sup>I</sup> complexes **14** ([**6**·Cu]ClO<sub>4</sub>) and **15** ([**6**·Cu]PF<sub>6</sub>), respectively, whereas red-colored complex **16** ([**12**·Cu]ClO<sub>4</sub>) was obtained from the reaction of **12** with [Cu(CH<sub>3</sub>CN)<sub>4</sub>]ClO<sub>4</sub>. Similarly, complexes **17** ([**6**·Ag]ClO<sub>4</sub>) and **18** ([**6**·Ag]PF<sub>6</sub>) were synthesized by the reaction of **6** with the corresponding silver salts. The reaction of **6** with Hg(OCOCH<sub>3</sub>)<sub>2</sub>/NH<sub>4</sub>PF<sub>6</sub> led to the formation of hydroxo-bridged complex **19**. The reaction of macrocycle **7** with Pd(C<sub>6</sub>H<sub>5</sub>CN)<sub>2</sub>Cl<sub>2</sub> gave access to novel complex **9a**. The macrocycles and the complexes have been characterized by elemental analysis, NMR (<sup>1</sup>H, <sup>13</sup>C, <sup>199</sup>Hg), fluorescence spectroscopy, and cyclic voltammetry. The molecular structures of organomercury precursors Hg{1-C<sub>6</sub>H<sub>4</sub>-2-(CH<sub>2</sub>OH)}<sub>2</sub> (**10**) and Hg{1-C<sub>6</sub>H<sub>4</sub>-2-(CHO)}<sub>2</sub> (**11**) and macrocycles **6**, **7**, and **12** show almost linear geometry around mercury; however, **13** shows a bent structure, i.e., significant deviation of the C–Hg–C angle from linearity. 22-Membered mercuraazametallamacrocycles **6**, **7**, and **12** are stabilized by secondary Hg···N intramolecular interaction and have an “hour-glass”-like conformation. The molecular structures of **14**, **17**, and **9a** showed metallophilic interactions. The metal ions (Cu<sup>I</sup> and Ag<sup>I</sup>) are coordinated not only to the four nitrogens but also to two mercury atoms, forming a distorted octahedral geometry around the metal ions.

## Introduction

Metallamacrocycles formed by the self-assembly of Lewis acids and bases have been studied extensively.<sup>1</sup> However, the metallamacrocycles, where the metal is embedded into the macrocycle in a preorganized framework through a covalent linkage, have received less attention. Only a few such examples have been reported in the literature. Generally, these

metallamacrocycles incorporate main group elements such as tin,<sup>2</sup> silicon,<sup>3</sup> boron,<sup>4</sup> germanium,<sup>5</sup> and mercury.<sup>6–12</sup> Among these, the polydentate organomercury macrocycles have attracted considerable current interest. The organomercury macrocycles include trimeric-perfluoro-*o*-phenylenemercury **1**,<sup>6</sup> [9]mercuracarborand-**3**,<sup>7</sup> [12]mercuracarborand-**4**,<sup>7</sup> a 24-membered macrocyclic perfluoroglutarate derivative,<sup>8a,b</sup>

\*To whom correspondence should be addressed. E-mail: chhbsia@chem.iitb.ac.in.

(1) (a) Newkome, G. R.; Wang, P.; Moorefield, C. N.; Cho, T. J.; Mohapatra, P. P.; Li, S.; Hwang, S.-H.; Lukyanova, O.; Echegoyen, L.; Palagallo, J. A.; Iancu, V.; Hla, S.-W. *Science* **2006**, *312*, 1782–1785. (b) Leininger, S.; Olenyuk, B.; Stang, P. J. *Chem. Rev.* **2000**, *100*, 853–908. (c) Gianneschi, N. C.; Masar, M. S., III; Mirkin, C. A. *Acc. Chem. Res.* **2005**, *38*, 825–837.

(2) (a) Newcomb, M.; Horner, J. H.; Blanda, M. T. *J. Am. Chem. Soc.* **1987**, *109*, 7878–7879. (b) Newcomb, M.; Blanda, M. T. *Tetrahedron Lett.* **1988**, *29*, 4261–4264. (c) Jurkschat, K.; Kuivila, H. G.; Liu, S.; Zubieta, J. A. *Organometallics* **1989**, *8*, 2755–2759.

(3) (a) Jung, M. E.; Xia, H. *Tetrahedron Lett.* **1988**, *29*, 297–300. (b) Suginome, M.; Oike, H.; Shuff, P. H.; Ito, Y. *Organometallics* **1996**, *15*, 2170–2178.

(4) (a) Jacobson, S.; Pizer, R. *J. Am. Chem. Soc.* **1993**, *115*, 11216–11221. (b) Jäkle, F. *Coord. Chem. Rev.* **2006**, *250*, 1107–1121.

(5) (a) Aoyagi, S.; Tanaka, K.; Zicmane, I.; Takeuchi, Y. *J. Chem. Soc., Perkin Trans. 2* **1992**, 2217–2220. (b) Aoyagi, S.; Tanaka, K.; Takeuchi, Y. *J. Chem. Soc., Perkin Trans. 2* **1994**, 1549–1553.

(6) (a) Sartori, P.; Golloch, A. *Chem. Ber.* **1968**, *101*, 2004–2009. (b) For review see: Haneline, M. R.; Taylor, R. E.; Gabbaï, F. P. *Chem.—Eur. J.* **2003**, *9*, 5188–5193.

(7) Wedge, T. J.; Hawthorne, M. F. *Coord. Chem. Rev.* **2003**, *240*, 111–128, and references therein.

(8) (a) Wuest, J. D. *Acc. Chem. Res.* **1999**, *32*, 81–89. (b) Wuest, J. D.; Zacharie, B. *J. Am. Chem. Soc.* **1987**, *109*, 4714–4715. (c) Vaugois, J.; Simard, M.; Wuest, J. D. *Organometallics* **1998**, *17*, 1215–1219.

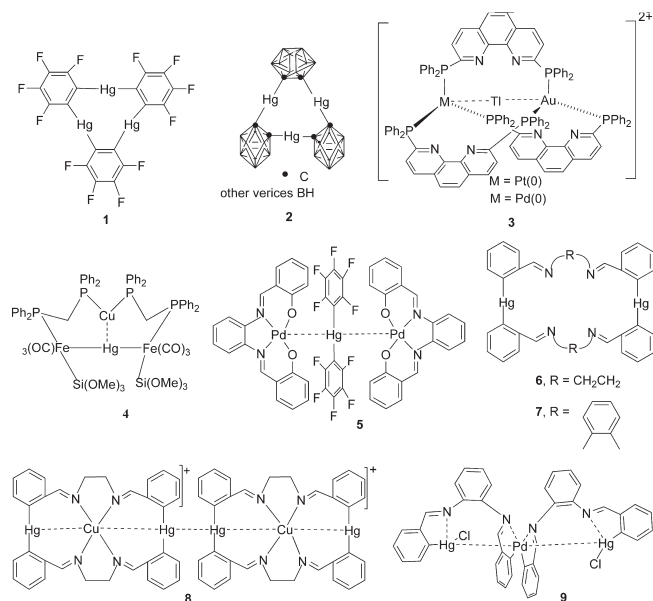
(9) Antipin, M. Yu.; Struchkov, Yu. T.; Volkonskii, A. Yu.; Rokhlin, E. M. *Izv. Akad. Nauk SSSR Ser. Khim.* **1983**, *2*, 452–455.

(10) (a) Badr, I. H. A.; Johnson, R. D.; Diaz, M.; Hawthorne, M. F.; Bachas, L. G. *Anal. Chem.* **2000**, *72*, 4249–4254. (b) Su, C.-Y.; Goforth, A. M.; Smith, M. D.; zur Loye, H.-C. *Inorg. Chem.* **2003**, *42*, 5685–5692.

(11) Lee, H.; Diaz, M.; Hawthorne, M. F. *Tetrahedron Lett.* **1999**, *40*, 7651–7655.

(12) Beer, P. D.; Smith, D. K. *Prog. Inorg. Chem.* **1997**, *46*, 1–96.

and a cyclic pentameric  $[(CF_3)_2CHg]_5$  macrocycle.<sup>9</sup> Due to the electrophilic nature of the metal ions, mercuramacrocycles act as sensors,<sup>10</sup> catalysts,<sup>11</sup> and anion receptors.<sup>12</sup> The binding of electron-rich species, e.g., anions,<sup>7–12</sup> solvent molecules, arenes, and alkynes with Lewis acidic mercuramacrocycles has been extensively investigated by Gabbai and co-workers and others.<sup>13,14</sup>



The interaction of metal ions with these metallamacrocycles would normally be expected to be repulsive due to the electrostatic repulsion between the positively charged metal ions. However, recent experimental and theoretical investigations have revealed the presence of weak metal...metal

interactions between both chemically similar and different closed-shell metal ions. Compounds with closed-shell  $d^{10}-d^{10}/d^8/s^2$  interactions have attracted considerable current interest because of their novel mode of bonding, structures, and unusual chemical and physical properties.<sup>15</sup> The types of forces that are involved in the binding of closed-shell atoms/ions have been a subject of considerable debate. Theoretical studies suggest that the dispersion forces magnified by relativistic effects<sup>16</sup> play a crucial role when these heavy closed-shell metal ions or atoms are involved in interactions. The nature of these weak interactions has also been interpreted in terms of an acid–base or donor–acceptor interaction.<sup>17</sup> As compared to the homometallic<sup>18</sup> closed-shell interactions, heterometallic interactions are rare.<sup>19</sup> Furthermore, there are relatively very few of them that contain three or more consecutive closed-shell ions/atoms.<sup>16</sup> In this regard the contributions by the groups of Catalano,<sup>20</sup> Braunstein,<sup>21</sup> and Gabbai<sup>17</sup> are notable. Catalano and co-workers<sup>20</sup> have reported encapsulation of metal ions or atoms in metallocryptands (**3**). These are formed by self-assembly, resulting in different types of closed-shell  $d^{10}\cdots d^{10}$  interactions. Braunstein and co-workers<sup>21</sup> have demonstrated the capture of metal ions/atoms by a heterometallogand (**4**) leading to heterometallic  $d^{10}\cdots d^{10}$  interactions. Gabbai and co-workers have recently reported a  $Pd^{II}\cdots Hg^{II}\cdots Pd^{II}$  closed-shell interaction, which is formed by a  $d^8\cdots d^{10}$  intermolecular interaction (**5**).<sup>17</sup>

We envisaged that if the mercuramacrocycles contained several strong Lewis base donors in addition to the Lewis acidic organomercury, the metalloligands could prove suitable hosts for the closed-shell  $d^{10}/d^8$  metal ions and may lead to heterometallic systems with metal...metal interaction. The attractive interaction of the bases with the guest metal ions should facilitate interaction of the guest ions with metal atoms of the host metallamacrocycle. Accordingly, we designed and synthesized mercurazamacrocycle **6**. The  $Cu^I$  complex of **6** exhibited two types of  $d^{10}\cdots d^{10}$  interaction: homophilic  $Hg^{II}\cdots Hg^{II}$  and heterophilic  $Hg^{II}\cdots Cu^I$  in a nearly linear chain of six  $d^{10}$  ions (**8**).<sup>22a</sup> Attempts to coordinate

(13) (a) Tsunoda, M.; Gabbai, F. P. *J. Am. Chem. Soc.* **2000**, *122*, 8335–8336. (b) King, J. B.; Haneline, M. R.; Tsunoda, M.; Gabbai, F. P. *J. Am. Chem. Soc.* **2002**, *124*, 9350–9351. (c) Haneline, M. R.; Tsunoda, M.; Gabbai, F. P. *J. Am. Chem. Soc.* **2002**, *124*, 3737–3742. (d) Omary, M. A.; Kassab, R. M.; Haneline, M. R.; Elbjerrami, O.; Gabbai, F. P. *Inorg. Chem.* **2003**, *42*, 2176–2178. (e) Tsunoda, M.; Gabbai, F. P. *J. Am. Chem. Soc.* **2003**, *125*, 10492–10493. (f) Taylor, T. J.; Burrell, C. N.; Gabbai, F. P. *Organometallics* **2007**, *26*, 5252–5263.

(14) Tikhonova, I. A.; Dolgushin, F. M.; Tugashov, K. I.; Petrovskii, P. V.; Furin, G. G.; Shur, V. B. *J. Organomet. Chem.* **2002**, *654*, 123–131, and references therein.

(15) (a) Dedieu, A.; Hoffmann, R. *J. Am. Chem. Soc.* **1978**, *100*, 2074–2079. (b) Pyykkö, P. *Chem. Rev.* **1997**, *97*, 597–636. (c) Pyykkö, P.; Mendizabal, F. *Inorg. Chem.* **1998**, *37*, 3018–3025. (d) Hermann, H. L.; Boche, G.; Schwerdtfeger, P. *Chem.—Eur. J.* **2001**, *7*, 5333–5342. (e) Mendizabal, F.; Pyykkö, P.; Runeberg, N. *Chem. Phys. Lett.* **2003**, *370*, 733–740. (f) Hakala, M. O.; Pyykkö, P. *Chem. Commun.* **2006**, 2890–2892.

(16) Thayer, J. S. *J. Chem. Educ.* **2005**, *82*, 1721–1727.

(17) Kim, M.; Taylor, T. J.; Gabbai, F. P. *J. Am. Chem. Soc.* **2008**, *130*, 6332–6333.

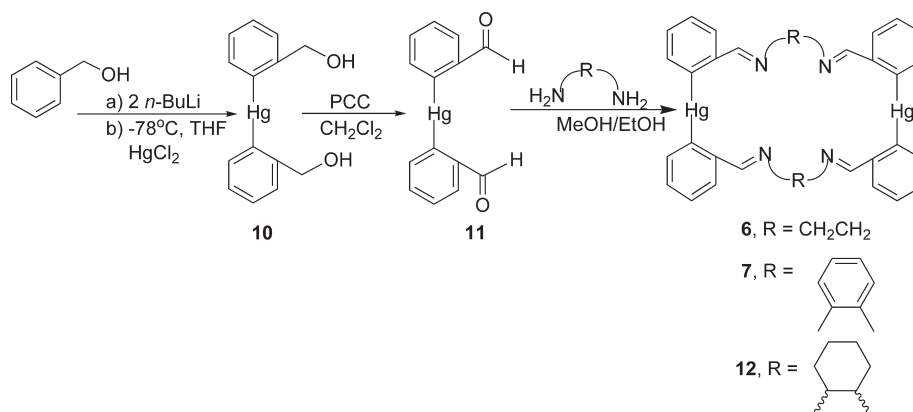
(18) (a) Fung, E. Y.; Olmstead, M. M.; Vickery, J. C.; Balch, A. L. *Coord. Chem. Rev.* **1998**, *171*, 151–159. (b) Ford, P. C.; Cariati, E.; Bourassa, J. *Chem. Rev.* **1999**, *99*, 3625–3647. (c) Yam, V. W.-W.; Lo, K. K.-W. *Chem. Soc. Rev.* **1999**, *28*, 323–334. (d) Fernández, E. J.; Gimeno, M. C.; Laguna, A.; López-de-Luzuriaga, J. M.; Monge, M.; Pyykkö, P.; Sundholm, D. *J. Am. Chem. Soc.* **2000**, *122*, 7287–7293. (e) Rawashdeh-Omary, M. A.; Omary, M. A.; Fackler, J. P., Jr. *J. Am. Chem. Soc.* **2001**, *123*, 9689–9691. (f) Hayashi, A.; Olmstead, M. M.; Attar, S.; Balch, A. L. *J. Am. Chem. Soc.* **2002**, *124*, 5791–5795. (g) Dias, H. V. R.; Diyalanage, H. V. K.; Rawashdeh-Omary, M. A.; Franzman, M. A.; Omary, M. A. *J. Am. Chem. Soc.* **2003**, *125*, 12072–12073. (h) Omary, M. A.; Mohamed, A. A.; Rawashdeh-Omary, M. A.; Fackler, J. P., Jr. *Coord. Chem. Rev.* **2005**, *249*, 1372–1381. (i) Barbieri, A.; Accorsi, G.; Armaroli, N. *Chem. Commun.* **2008**, 2185–2193. (j) Bravo, J.; Casas, J. S.; Mascarenhas, Y. P.; Sanchez, A.; Santos, C. de O. P.; Sordo, J. J. *Chem. Soc., Chem. Commun.* **1986**, 1100–1101.

(19) (a) Burini, A.; Fackler, J. P., Jr.; Galassi, R.; Grant, T. A.; Omary, M. A.; Rawashdeh-Omary, M. A.; Pietroni, B. R.; Staples, R. J. *J. Am. Chem. Soc.* **2000**, *122*, 11264–11265. (b) Józsa, R.; Beszedi, I.; Bényei, A. C.; Fischer, A.; Kovács, M.; Maliarik, M.; Nagy, P.; Shchukarev, A.; Tóth, I. *Inorg. Chem.* **2005**, *44*, 9643–9651. (c) Falvello, L. R.; Fornies, J.; Martín, A.; Navarro, R.; Sicilia, V.; Villarroja, P. *Inorg. Chem.* **1997**, *36*, 6166–6171. (d) Laguna, M.; Villacampa, M. D.; Contel, M.; Garrido, J. *Inorg. Chem.* **1998**, *37*, 133–135. (e) Knoepfler, A.; Wurst, K.; Peringer, P. *J. Chem. Soc., Chem. Commun.* **1995**, 131–132. (f) Weil, M.; Tillmanns, E.; Pushcharovsky, D. Y. *Inorg. Chem.* **2005**, *44*, 1443–1451.

(20) (a) Catalano, V. J.; Bennett, B. L.; Kar, H. M.; Noll, B. C. *J. Am. Chem. Soc.* **1999**, *121*, 10235–10236. (b) Catalano, V. J.; Bennett, B. L.; Noll, B. C. *Chem. Commun.* **2000**, 1413–1414. (c) Catalano, V. J.; Bennett, B. L.; Yson, R. L.; Noll, B. C. *J. Am. Chem. Soc.* **2000**, *122*, 10056–10062. (d) Catalano, V. J.; Bennett, B. L.; Muratidis, S.; Noll, B. C. *J. Am. Chem. Soc.* **2001**, *123*, 173–174. (e) Catalano, V. J.; Malwitz, M. A.; Noll, B. C. *Chem. Commun.* **2001**, 581–582. (f) Catalano, V. J.; Malwitz, M. A.; Noll, B. C. *Inorg. Chem.* **2002**, *41*, 6553–6559. (g) Catalano, V. J.; Bennett, B. L.; Malwitz, M. A.; Yson, R. L.; Kar, H. M.; Muratidis, S.; Horner, S. J. *Comments on Inorg. Chem.* **2003**, *24*, 39–68. (h) Catalano, V. J.; Malwitz, M. A.; Etogo, A. O. *Inorg. Chem.* **2004**, *43*, 5714–5724. (i) Catalano, V. J.; Malwitz, M. A. *J. Am. Chem. Soc.* **2004**, *126*, 6560–6561.

(21) (a) Bodensieck, U.; Braunstein, P.; Knorr, M.; Strampfer, M.; Bénard, M.; Strohmann, C. *Angew. Chem., Int. Ed.* **1997**, *36*, 2758–2761. (b) Schuh, W.; Braunstein, P.; Bénard, M.; Rohmer, M.-M.; Welter, R. *Angew. Chem., Int. Ed.* **2003**, *42*, 2161–2164. (c) Braunstein, P.; Frison, C.; Oberbeckmann-Winter, N.; Morise, X.; Messaoudi, A.; Bénard, M.; Rohmer, M.-M.; Welter, R. *Angew. Chem., Int. Ed.* **2004**, *43*, 6120–6125. (d) Schuh, W.; Braunstein, P.; Bénard, M.; Rohmer, M.-M.; Welter, R. *J. Am. Chem. Soc.* **2005**, *127*, 10250–10258.

Scheme 1. Synthetic Route to the Macrocycles 6, 7, and 12

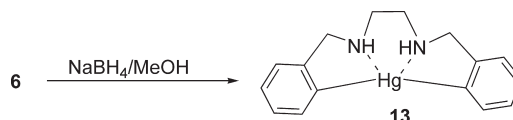


the  $\text{Pd}^{\text{II}}$  ion with **7** led to a facile transmetalation and the formation of a novel helical trimetallic complex (**9**) with a  $\text{Hg}^{\text{II}} \cdots \text{Pd}^{\text{II}} \cdots \text{Hg}^{\text{II}}$  interaction.<sup>22b</sup> Extending the concept, we now report the synthesis and characterization of some new Schiff base metallophillic mercurazamacrocycles and their metal complexes with  $\text{Cu}^{\text{I}}$ ,  $\text{Ag}^{\text{I}}$ ,  $\text{Pd}^{\text{II}}$ , and  $\text{Pt}^{\text{II}}$  that exhibit  $d^{10} \cdots d^{10}/d^{10} \cdots d^8$  interactions. In particular, we draw attention to  $\text{Hg}^{\text{II}} \cdots \text{Ag}^{\text{I}} \cdots \text{Hg}^{\text{II}}$  as a closed-shell interaction involving three atoms in a colinear bond with short internuclear distances. The metal  $\cdots$  metal interactions have been confirmed by X-ray crystallography. We also describe our attempts to synthesize the a trimetallic complex with a  $\text{Hg}^{\text{II}} \cdots \text{Hg}^{\text{II}} \cdots \text{Hg}^{\text{II}}$  closed-shell interaction, which furnished a cleaved compound with a  $\text{Hg}-\text{O}-\text{Hg}$  bond. The reduction of the mercurazamacrocycle **6** with  $\text{NaBH}_4$  is shown to furnish an 11-membered mercurazamacrocycle, unprecedented in its  $\text{C}-\text{Hg}-\text{C}$  angle of  $135.5^\circ$ .

## Results and Discussion

Synthesis of the mercurazamacrocycles and their precursors is outlined in Scheme 1. Benzyl alcohol, upon lithiation followed by the reaction with  $\text{HgCl}_2$  at  $-78^\circ\text{C}$ , gave bis(*o*-hydroxymethylphenyl)mercury (**10**). Bis(*o*-formylphenyl)mercury (**11**) was obtained by the oxidation of **10** with PCC (pyridinium chlorochromate). The synthesis of **11** has been earlier reported by Flower et al.<sup>23</sup> and Rickard et al.<sup>24</sup> by slightly different routes. In our modification, coupling of the organomercury halide with  $\text{NaI}$  and protection of the alcohol groups is avoided. In an attempt to synthesize the mercurous analogue of **11**, when the lithiated benzyl alcohol was reacted with  $\text{Hg}_2\text{Cl}_2$ , the reaction afforded only **10**. Reactions of 1,2-diaminoethane, 1,2-diaminobenzene, and *trans*-1,2-diaminocyclohexane with **11** afforded ligands **6**, **7**, and **12**, respectively, in good yields without recourse to a metal ion template or high dilution techniques. The synthesis of macrocycle **7** required refluxing, whereas **6** and **12** formed at room temperature. Secondary intramolecular  $\text{Hg} \cdots \text{N}$  coordination (vide infra) plays an important role in the formation of the (2 + 2) macrocycles. In general, all these compounds show poor solubility in solvents such as pentane

Scheme 2. Synthesis of 11-Membered Mercurazamacrocycle 13



and hexane; however, they were highly soluble in chloroform and dichloromethane and moderately soluble in acetone, acetonitrile, DMSO, and DMF.

In order to get a more stable and flexible tetraamino derivative of **6**, its reduction with an excess of  $\text{NaBH}_4$  was attempted. The reduction resulted in the formation of an unexpected reduced macrocycle, **13** (Scheme 2). The 11-membered macrocycle presumably results from the cleavage of the  $\text{Hg}-\text{C}$  bond during reduction. This type of demercuration and skeletal rearrangement have been earlier observed in the reduction of organomercury compounds.<sup>25</sup> Compound **13** was recrystallized from a dichloromethane and hexane mixture as square-shaped crystals. The IR and  $^1\text{H}$ ,  $^{13}\text{C}$  and  $^{199}\text{Hg}$  NMR spectroscopic data confirm the total reduction of the Schiff base macrocycle. ESI-MS and X-ray crystallographic studies (vide infra) unambiguously establish the formation of the 11-membered reduced macrocycle with a significantly bent  $\text{C}-\text{Hg}-\text{C}$  angle (see Figure 6).

The reaction of ligand **6** with  $\text{Cu}(\text{CH}_3\text{CN})_4\text{ClO}_4$  and  $\text{Cu}(\text{OCOCH}_3)_2/\text{NH}_4\text{PF}_6$  afforded orange-colored  $\text{Cu}^{\text{I}}$  complexes **14** ( $[\text{6} \cdot \text{Cu}^{\text{I}}]\text{ClO}_4$ ) and **15** ( $[\text{6} \cdot \text{Cu}^{\text{I}}]\text{PF}_6$ ) (Scheme 3).<sup>22a</sup> The reaction of ligand **12** with  $\text{Cu}(\text{CH}_3\text{CN})_4\text{ClO}_4$  in a 1:1 ratio under nitrogen gave the red-colored complex **16** ( $[\text{12} \cdot \text{Cu}^{\text{I}}]\text{ClO}_4$ ), which showed a base peak at  $m/z$  1041 corresponding to  $[\text{M} - \text{ClO}_4]^+$  in the ES-MS. Complex **16** is soluble in chloroform and dichloromethane. Upon addition of solvents such as acetonitrile, acetone, DMF, and DMSO, the complex decomposes to give a white residue. Complexes **14**, **15**, and **16** are soluble in acetonitrile. The reaction of ligand **6** with  $\text{AgClO}_4$  or  $\text{AgNO}_3/\text{NH}_4\text{PF}_6$  afforded complexes **17** ( $[\text{6} \cdot \text{Ag}^{\text{I}}]\text{ClO}_4$ ) and **18** ( $[\text{6} \cdot \text{Ag}^{\text{I}}]\text{PF}_6$ ), respectively. In the ES-MS both the complexes exhibited a peak at  $m/z$  977 corresponding to  $[\text{M} - \text{X}]^+$  ( $\text{X} = \text{ClO}_4^-$ ,  $\text{PF}_6^-$ ). The reactions of  $\text{Cu}^{\text{II}}$  and  $\text{Ag}^{\text{I}}$  salts with **12** were unsuccessful. Although the cavity size of **12** is nearly the same as that of **6**, the conformational constraints introduced by use of a cyclic diamine may prevent coordination of  $\text{Ag}^{\text{I}}$  with **12**. It is interesting to note

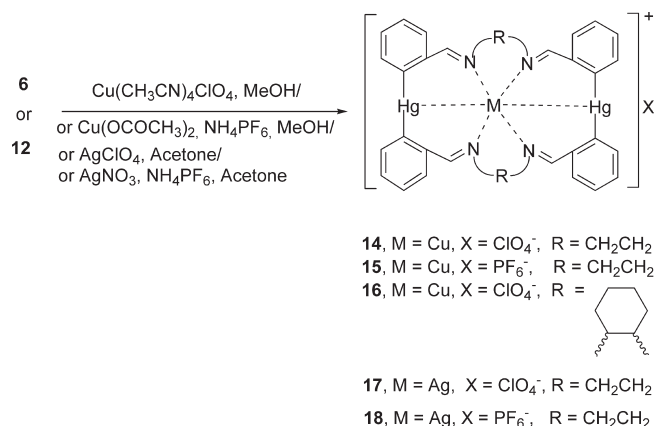
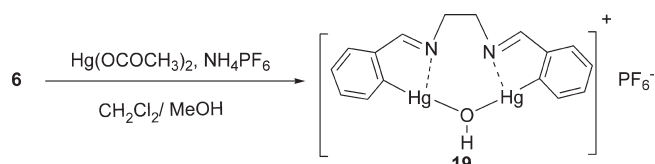
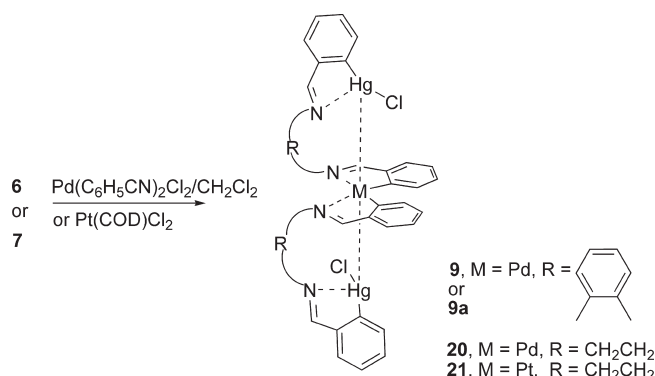
(22) (a) Patel, U.; Singh, H. B.; Wolmershäuser, G. *Angew. Chem., Int. Ed.* **2005**, *44*, 1715–1717. (b) Sharma, S.; Baligar, R. S.; Singh, H. B.; Butcher, R. J. *Angew. Chem., Int. Ed.* **2009**, *48*, 1987–1990.

(23) Flower, K. R.; Howard, V. J.; Naguthney, S.; Pritchard, R. G.; Warren, J. E.; McGown, A. T. *Inorg. Chem.* **2002**, *41*, 1907–1912.

(24) Rickard, C. E. F.; Roper, W. R.; Tutone, F.; Woodgate, S. D.; Wright, L. J. *J. Organomet. Chem.* **2001**, *619*, 293–298.

(25) (a) Gouzoules, F. H.; Whitney, R. A. *Tetrahedron Lett.* **1985**, *26*, 3441–3444, and references therein. (b) Kang, S. H.; Lee, J. H.; Lee, S. B. *Tetrahedron Lett.* **1998**, *39*, 59–62.



Scheme 3. Synthesis of Cu<sup>I</sup> and Ag<sup>I</sup> Complexes of **6** and **12**Scheme 4. Synthesis of Hydroxo-Bridged Compound **19**Scheme 5. Synthesis of **9/9a**, **20**, and **21**

that the reaction of **6** with Cu<sup>II</sup> afforded the reduced Cu<sup>I</sup> complex and not the expected Cu<sup>II</sup> complex. This reduction is probably accompanied by the oxidation of methanol present in the system to either formaldehyde or formic acid; however, attempts to characterize the oxidized species were not successful. Lai and co-workers<sup>26</sup> have observed a similar reduction of a Cu<sup>II</sup> ion when treated with a quinquedentate macrocycle, and they suggested that the autoreduction was due to the electron-donating properties of the ligand or the geometry of the complex formed.

A similar reaction of Hg(OCOCH<sub>3</sub>)<sub>2</sub>/NH<sub>4</sub>PF<sub>6</sub> with **6** to get the Hg<sup>II</sup> analogue, with a Hg<sup>II</sup>...Hg<sup>II</sup>...Hg<sup>II</sup> interaction, led to the cleavage of the macrocycle to give the cationic complex **19**, where the hydroxide ion is bridged between the two mercury atoms (Scheme 4). In view of the identical mass and number of electrons for hydroxide ion and fluoride ion, the possibility of the fluoro-bridged complex was also considered. However, this could be ruled out on the basis of the <sup>19</sup>F NMR spectrum, which showed only one peak for the PF<sub>6</sub><sup>−</sup> anion.

Table 1. <sup>199</sup>Hg NMR Chemical Shifts (in ppm) of Synthesised Compounds

compound	<sup>199</sup> Hg NMR	compound	<sup>199</sup> Hg NMR
Ph <sub>2</sub> Hg	−745 <sup>a</sup>	<b>14</b>	−559 <sup>b</sup>
Ph <sub>2</sub> Hg	−806 <sup>b</sup>	<b>15</b>	−537 <sup>c</sup>
<b>10</b>	−690 <sup>b</sup>	<b>16</b>	−495 <sup>a</sup>
<b>11</b>	−750 <sup>a</sup>	<b>17</b>	−552 <sup>c</sup>
<b>6</b>	−690 <sup>a</sup>	<b>18</b>	−555 <sup>c</sup>
<b>12</b>	−667 <sup>a</sup>	<b>19</b>	−1013 <sup>b</sup>
<b>7</b>	−750 <sup>a</sup>	<b>20</b>	−1045 <sup>b</sup>
<b>13</b>	−572 <sup>a</sup>	<b>21</b>	−1043 <sup>b</sup>

<sup>a</sup> CDCl<sub>3</sub>. <sup>b</sup> d<sub>6</sub>-DMSO. <sup>c</sup> CD<sub>3</sub>CN.

The reactions of macrocycles **6** and **7** with Pd(C<sub>6</sub>H<sub>5</sub>CN)<sub>2</sub>-Cl<sub>2</sub>/Pt(COD)Cl<sub>2</sub> in dichloromethane led to the formation of trimetallic complexes **20**, **21**, and **9**, respectively, having Hg<sup>II</sup>...Pd<sup>II</sup>/Pt<sup>II</sup>...Hg<sup>II</sup> interactions (Scheme 5).<sup>22b</sup> The ES-MS spectra of **20** and **21** showed peaks for [M − Cl]<sup>+</sup> at *m/z* 1011 and 1100, respectively. The recrystallization of **9** with acetone gave a pseudopolymorph (**9a**) of the complex. All the complexes are quite stable in air. However, these are stable only for a few days in solution, after which they begin to decompose.

In solution, the ligands and the complexes were characterized by UV-vis, fluorescence, cyclic voltammetry, and detailed NMR (<sup>1</sup>H, <sup>13</sup>C, <sup>199</sup>Hg) studies. The <sup>199</sup>Hg NMR data for all the compounds are given in Table 1 and are reported relative to diphenyl mercury as external standard (−745 ppm). The <sup>199</sup>Hg NMR chemical shifts are sensitive to the solvent and also to the electronic and steric substituents on mercury.<sup>27</sup> The <sup>199</sup>Hg signals for the ligands **10**, **6**, and **12** are shifted downfield relative to Ph<sub>2</sub>Hg. This shift may be attributed to the +I effect of −CH<sub>2</sub>OH and the imino groups. A weak intramolecular Hg...O/N interaction is also possible in solution (vide infra). In the case of the imine derivatives **6** and **12**, such interactions are quite prominent in the solid state. Although the structure of **11** indicates a weak interaction between −CHO and Hg, in the solid state (vide infra), the <sup>199</sup>Hg NMR data are not indicative of any significant Hg...OCH interaction. This may be due to two opposing effects, viz., the −I of −CHO and an intramolecular Hg...O interaction. Interestingly, the <sup>199</sup>Hg signal for **13** is observed at ca. −572 ppm, which is downfield shifted by ~120 ppm with respect to the parent compound **6**, indicating a much stronger coordination between Hg and N. The structural analysis (vide infra) of **13** further supports a change in the coordination geometry around Hg with the formation of strong Hg−N bonds. The <sup>199</sup>Hg NMR signal of **16** at −495 ppm is ~220 ppm upfield shifted as compared to the free ligand **12** (Table 1). Complexes **17** and **18** exhibited a single peak at around −552 ppm in the <sup>199</sup>Hg NMR spectra, whereas compound **19** showed a peak at −1013 ppm in the <sup>199</sup>Hg NMR spectrum. Also the <sup>199</sup>Hg NMR signals for **20** and **21** appear at −1045 and −1043 ppm, respectively (Table 1). Such a large downfield shift in the <sup>199</sup>Hg NMR with respect to the simple metal complexes **14**–**16** is indicative of the formation of organomercury chloride. However, such a downfield shift in a polar solvent such as DMSO-*d*<sub>6</sub> should be taken with caution, as the observed chemical shift differences may be also due to the coordination of polar solvent molecules to the Hg atom in solution.

(26) Vetrichelvan, M.; Lai, Y.; Mok, K. F. *Dalton Trans.* **2003**, 295–303.

(27) Wrackmeyer, B.; Contreras, R. *Annu. Rep. NMR Spectrosc.* **1992**, 24, 267–329.

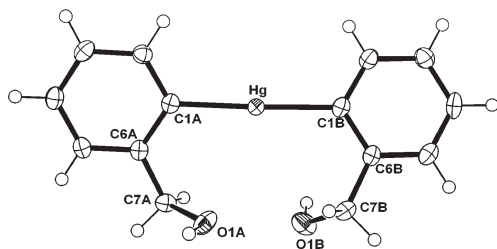


**Figure 1.** Crystal structure of **10** (50% ellipsoids). Selected bond lengths (Å) and angles (deg): Hg–C1B 2.085(4), Hg–C1A 2.089(4), Hg–O1A 3.098(4), Hg–O1B 3.232(4), C1B–Hg–C1A 177.88(16).

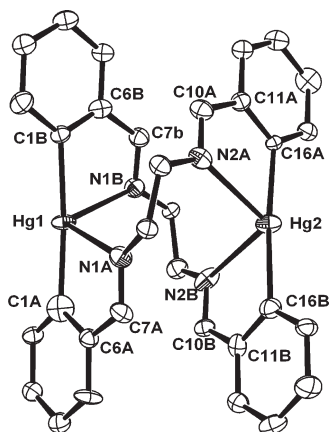


**Figure 2.** Crystal structure of **6** (50% ellipsoids, H atoms omitted for clarity). Selected bond lengths (Å) and angles (deg): Hg1–N1B 2.65(2), Hg1–N1A 2.70(2), Hg2–N2B 2.65(3), Hg2–N2A 2.72(2), C1A–Hg1–C1B 175.2(7), C16A–Hg2–C16B 175.1(7), N1A–Hg1–N1B 107.6(7), N2A–Hg2–N2B 108.6(7).

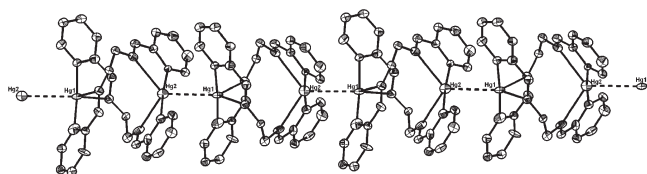


**Figure 3.** Packing diagram of **6** showing intramolecular Hg...Hg interaction.

The electronic spectra of macrocycles **6**, **7**, **12**, and **13** and the complexes were recorded in solution and in the solid state. In solution the macrocycles exhibit a high-energy feature at  $\sim 290$  nm corresponding to the  $\pi$ – $\pi^*$  transition. Macrocycle **7** shows an additional absorption at 375 nm corresponding to the  $n$ – $\pi^*$  transition. In the solid state **6**, **12**, and **13** exhibit a  $\pi$ – $\pi^*$  absorption at  $\sim 336$  nm, whereas **7** shows an absorption at 418 nm. Similar to the copper complexes of **6**,<sup>22a</sup> complex **16** also shows a metal to ligand charge-transfer band at 450 nm in solution and at 475 nm in the solid state in addition to the high-energy transition at  $\sim 336$  nm. Palladium complex **20** has a broad absorption in the range 460–489 nm in the solid state. Macrocycles **6**, **7**, and **12** are found to be luminescent. Macrocycles **6** and **12**, upon excitation at 336 nm, show emission peaks at 422, 460, and 530 nm in the solid state. Macrocycle **7** shows strong emission peaks at 484 and 524 nm when excited at 418 nm.

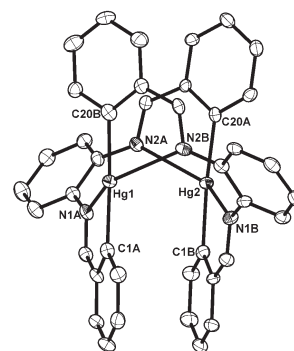


**Figure 4.** Crystal structure of **7** (50% ellipsoids, H atoms omitted for clarity). Selected bond lengths (Å) and angles (deg): Hg1–C1A 2.079(5), Hg1–C20B 2.073(5), Hg1–N1A 2.750(4), Hg2–N1B 2.760(4), C1A–Hg1–C20B 177.4(2), C1B–Hg2–C20A 175.07(19), C20A–Hg2–N2A 71.93(17), C20A–Hg2–N1B 109.08(17), N2A–Hg2–N1B 143.35(12).

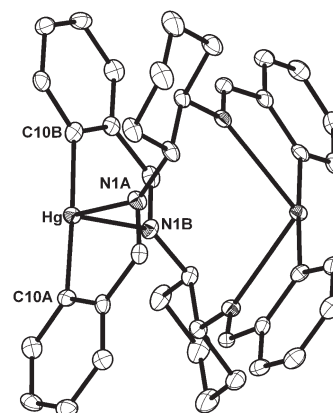


**Figure 5.** Crystal structure of **12** (50% ellipsoids, H atoms omitted for clarity). Selected bond lengths (Å) and angles (deg): Hg–C10A 2.077(3), Hg–C10B 2.077(3), Hg–N1A 2.676(3), Hg–N1B 2.716(2), C10A–Hg–C10B 177.89(11), C10A–Hg–N1A 74.49(10), C10A–Hg–N1B 108.20(9), N1A–Hg–N1B 109.51(7).

For complex **16**, by exciting at 475 nm in the solid state, the emission peak is obtained at 530 nm. The cyclic voltammetric study of **16** shows a quasi-reversible system with oxidation at 0.807 V and reduction at 0.476 V with a  $\Delta E$  of 0.331 V. The cyclic voltammogram of **17**, as expected for  $\text{Ag}^{\text{I}}$  complexes, shows irreversible oxidation at 0.364 V and reduction at 0.100 V with a  $\Delta E$  of 0.264 V, and for **18** the oxidation occurs at 0.124 V and reduction at 0.397 V, with a  $\Delta E$  of 0.273 V.

Molecular structures of **10**, **11**, **6**, **7**, **12**, **13**, **17**, **19**, and **9a** are depicted in Figures 1–11. Compounds **10** and **11** crystallized in the monoclinic crystal system and triclinic system, respectively. The C–Hg–C bond angles for **10** and **11** are almost linear, with bond angles of 177.88(16) $^\circ$  (Figure 1) and 179.0(6) $^\circ$ , respectively (Figure S25). Compound **10** exhibits weak intramolecular interactions between mercury and oxygen of the hydroxyl group with Hg...O distances of 3.098(4) and 3.232(4) Å, respectively. The distances are greater than the sum of the covalent radii;<sup>28</sup> however, these are close to the sum of the van der Waals radii of mercury (1.73–2.05 Å<sup>29a–c</sup>) and oxygen (1.52 Å<sup>29d</sup>). For compound **11**, the Hg1...O11 and Hg1...O12 distances are 2.870(14) and 2.855(14) Å,

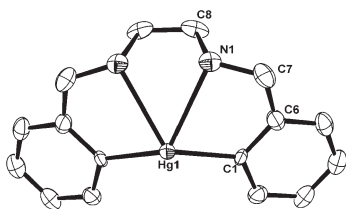


**Figure 6.** Crystal structure of **13** (50% ellipsoids). Selected bond lengths (Å) and angles (deg): Hg1–C1 2.079(7), Hg1–N1 2.684(5), C1–Hg1–C1 135.5(3), C1–Hg1–N1 125.57(17), N1–Hg1–N1 54.0(2).

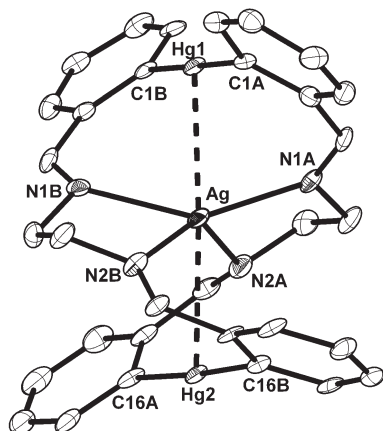


**Figure 7.** Crystal structure of cation **17** (50% ellipsoids, H atoms and anion omitted for clarity). Selected bond lengths (Å) and angles (deg): Hg1–Ag 2.8741(7), Hg2–Ag 2.9472(7), Ag–N1A 2.222(6), Ag–N1B 2.380(6), Ag–N2A 2.502(7), Ag–N2B 2.241(7), Hg1–Ag–Hg2 166.50(3), C1B–Hg1–C1A 178.9(3), C16A–Hg2–C16B 176.3(3).

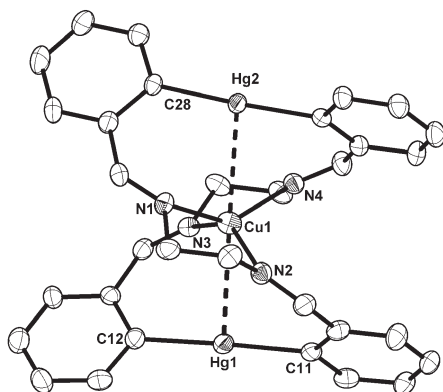


**Figure 8.** Crystal structure of cation **14** (30% ellipsoids, H atoms and anion omitted for clarity). Selected bond lengths (Å) and angles (deg): Hg1–Cu1 2.9212(7), Hg2–Cu1 2.9198(7), Cu1–N1 2.114(4), Cu1–N2 2.071(5), Cu1–N3 2.100(4), Cu1–N(4) 2.062(4), Hg2–Cu1–Hg1 177.88(3), C27–Hg2–C28 177.23(18), C11–Hg1–C12, 177.80(18).

respectively, which are comparable to the reported value of 2.827(7) Å for  $\text{HgCl}\{1\text{-C}_6\text{H}_4\text{-2-(CHO)}\}$  (for details see Figure S25 in the Supporting Information).<sup>24</sup>

(28) Cordero, B.; Gómez, V.; Platero-Prats, A. E.; Revés, M.; Echeverría, J.; Cremades, E.; Barragán, F.; Alvarez, S. *Dalton Trans.* **2008**, 2832–2838.

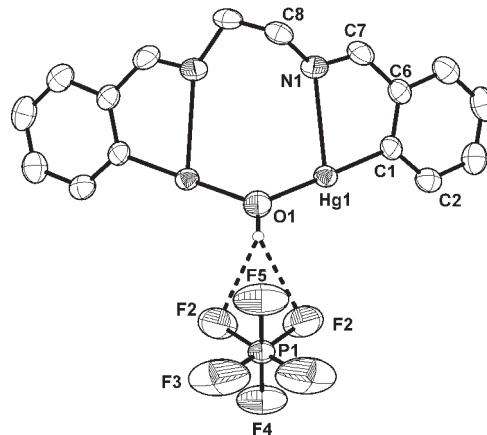


**Figure 9.** Crystal structure of cation **19** (50% ellipsoids, H atoms and anion omitted for clarity). Selected bond lengths (Å) and angles (deg): Hg1–C1, 2.042(8), Hg1–N1 2.669(8), Hg1–O1 2.069(6), Hg1–O1–Hg1 109.3(4), C1–Hg1–N1 74.9(3), C1–Hg1–O1 178.5(3).

Mercuraazamacrocyclic **6** crystallizes in the monoclinic crystal system. To our knowledge, this is the first single-crystal X-ray structure (Figure 2) of a metallamacrocyclic containing covalently linked mercury and nitrogen in its molecular framework. The geometry about each mercury atom is nearly linear. The  $\angle\text{C1A–Hg1–C1B}$  ( $175.2(7)^\circ$ ) is only slightly deviated from linearity. The notable feature of the molecular structure is the presence of the intramolecular interaction of the imine nitrogens with the Hg1 and Hg2 atoms. All four nitrogen atoms interact with the two mercury atoms, having bond distances [Hg1–N1B 2.65(2) Å, Hg1–N1A 2.70(2) Å, Hg2–N2B 2.65(3) Å and Hg2–N2A 2.72(2) Å] that are much less than the sum of the van der Waals radii,<sup>29</sup> but close to the sum of covalent radii, i.e., 2.03 Å (Hg 1.32 + N 0.71 Å).

The observed Hg–N distances are shorter than the Hg–N distance observed for related acyclic Schiff base compounds of **11** with aromatic monoamines (2.85–2.71 Å).<sup>23</sup> These are also less than the Hg–N distances (2.860–3.126 Å) observed in  $\sigma$ -alkynyl complexes of orthomercurated Schiff bases of substituted benzylideneanilines and anthracenylmethyleneanilines.<sup>30</sup> The Hg–N intramolecular interactions probably force the macrocycle into an “hour-glass” conformation. The transannular distance between two Hg atoms is 4.992(2) Å. The packing diagram reveals the presence of the intermolecular  $\text{d}^{10}\cdots\text{d}^{10}$  interaction between Hg1 and Hg2# (3.1643(14) Å) (Figure 3). This distance is longer than the intermolecular Hg $\cdots$ Hg distance of 3.101(2) Å reported for methyl(2-mercapto-4-methylpyrimidinato)mercury(II).<sup>18j,29b</sup>

Compound **7** crystallizes in the monoclinic crystal system and in the  $P2_1/c$  space group. One of the important features of the mercuracycle **7** is the short distance between Hg1 and Hg2, which is 3.654 Å (Figure 4).

The distance between Hg1 and Hg2 in **7** is much less than the Hg $\cdots$ Hg distance in **6** (4.992 Å) as well as in **12** (4.924 Å). All four nitrogen atoms strongly interact with the two mercury atoms, having bond distances Hg1 $\cdots$ N1A (2.750(4) Å),

(29) (a) Canty, A. J.; Deacon, G. B. *Inorg. Chim. Acta* **1980**, 45, L255–L227. (b) Pyykkö, P.; Straka, M. *Phys. Chem. Chem. Phys.* **2000**, 2, 2489–2493. (c) Batsanov, S. S. *Inorg. Mater.* **2001**, 36, 1031–1046. (d) Bondi, A. *J. Phys. Chem.* **1964**, 68, 441–451.

(30) Wong, W.-Y.; Lu, G.-L.; Liu, L.; Shi, J.-X.; Lin, Z. *Eur. J. Inorg. Chem.* **2004**, 2066–2077.

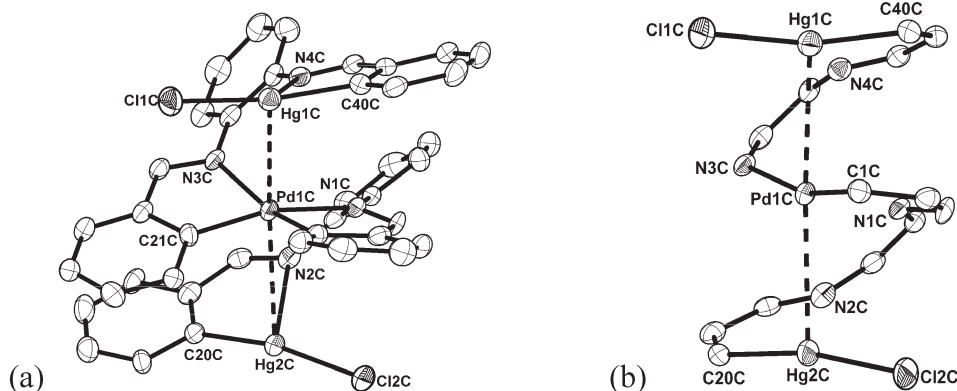


**Figure 10.** (a) Crystal structure of **9a** (50% ellipsoids, one of the molecules in the asymmetric unit is shown, H atoms and the other three molecules in the asymmetric unit are omitted for clarity). Selected bond lengths (Å) and angles (deg): Hg1C–Pd1C 3.1496(9), Hg2C–Pd1C 3.2201(9), Hg1C–N4C 2.777(9), Hg2C–N2C 2.663(10), Pd1C–N1C 2.158(8), Pd1C–N3C 2.178(11), Hg1C–Pd1C–Hg2C 162.22(3), C40C–Hg1C–Cl1C 165.8(3), C20C–Hg2C–Cl2C 168.3(4). (b) Simplified ORTEP picture of **9a** showing a helical structure.

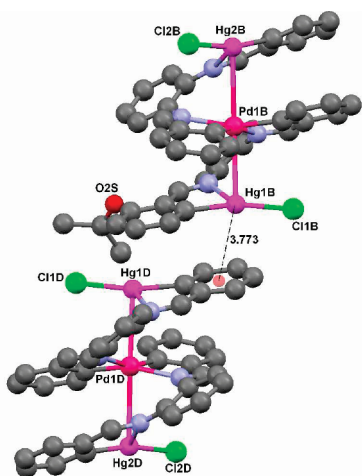


**Figure 11.** Hg $\cdots\pi$  interaction in acetone solvate of **9a**.

Hg1 $\cdots$ N2B (2.777(4) Å), Hg2 $\cdots$ N2A (2.772(4) Å), and Hg2 $\cdots$ N1B (2.760(4) Å). The C1A–Hg1–C20B bond angle is almost linear, at 177.4(2)°. The molecular structure depicts the mutual stacking of the phenyl rings attached to mercury atoms.

Macrocycle **12** crystallizes in the orthorhombic crystal system. Although the reaction of bis(*o*-formylphenyl)-mercury **11** with racemic *trans*-1,2-cyclohexane diamine can give product **12** as three different stereoisomers (viz., (*R,R*)-(*R,R*); (*S,S*)-(*S,S*); (*R,R*)-(*S,S*)), the crystal structure shows the presence of a 1:1 ratio of (*R,R*)-(*R,R*) and (*S,S*)-(*S,S*) isomers formed from the (*R,R*) and (*S,S*) enantiomers of the diamine, respectively. Here also the geometry around each Hg atom is nearly linear, with an intramolecular interaction between the imine nitrogen atoms and Hg atoms (Figure 5). All four nitrogens interact with the two mercury atoms, having bond distances Hg–N1B of 2.716(2) Å and Hg–N1A of 2.676(3) Å. The  $\angle$ C10A–Hg–C10B is almost linear (177.89(11)°). The deviation of the C–Hg–C angle from linearity is more in the case of **6** as compared to **12**. The transannular distance between the two Hg atoms is 4.924(0) Å.

Compound **13** crystallizes in the orthorhombic crystal system and space group *Cmc*<sub>21</sub>. The geometry around Hg is distorted tetrahedral, where Hg is coordinated to two sp<sup>3</sup>

nitrogen atoms (Figure 6). The most noteworthy feature of the structure is the nonlinearity of the geometry about mercury. In a recent review on Lewis acid behavior of organomercurials, Gabbai and co-workers<sup>13f</sup> have noted that a nearly linear C–Hg–C geometry in organomercury adducts indicates an extremely weak ligand $\rightarrow$ Hg interaction. This behavior has been interpreted in terms of the unfavorable energy of mercury orbitals for overlap with donor orbitals. The observed bond angle of C1–Hg1–C1 (135.5(3)°) in **13** deviates significantly from linearity and is the maximum observed for any diorganomercury derivative.

This deviation is significantly greater than the deviation observed for the chloride complex of [12]mercuracarborane-4 (162°).<sup>31</sup> In diorganomercury compounds, Hg<sup>II</sup> can be also considered as sp hybridized (although participation of d orbitals is also expected) and forms two linear covalent bonds while retaining two empty and mutually perpendicular p-orbitals. The two filled orbitals of two nitrogen atoms interact with the two empty orbitals of mercury. The Hg–N bond distance observed is 2.684(5) Å. Interestingly, the Hg–N distances are on the same order as those observed in macrocycles **6** and **12**. Thus, the significant deviation of the C–Hg–C bond angle in **13** may also be due to the small size of the ring. The deviation of the C–Hg–C bond from linearity requires mixing of some additional p-character into the sp-hybrid mercury orbitals involved in bonding to aromatic carbon atoms. The C7–N1 and C8–N1 bond distances are 1.460(9) and 1.487(10) Å, respectively, compared to the C=N bond distances,  $\sim$ 1.30 Å,<sup>28</sup> in **6**, confirming complete reduction of the C=N bonds. Compound **13** also exhibits a weak intramolecular C–H $\cdots$ Hg van der Waals interaction at a distance (3.131 Å) close to the sum of the van der Waals radii of Hg and H.

Complex **17** crystallizes in the monoclinic crystal system. The silver ion is coordinated to four nitrogen and two mercury atoms of the macrocycle, forming a distorted octahedral geometry (Figure 7). To our knowledge, this is the first structural example of the encapsulation of a silver ion in a metallamacrocycle cavity. In the literature there are very

(31) Yang, X.; Knobler, C. B.; Hawthorne, M. F. *Angew. Chem., Int. Ed. Engl.* **1991**, 30, 1507–1508.



few reports of a six-coordinated  $\text{Ag}^{\text{I}}$  ion.<sup>32</sup> The  $\text{Hg1}-\text{Ag}-\text{Hg2}$  bond angle is  $166.50(3)^\circ$  and deviates from linearity. The  $\text{Hg1}\cdots\text{Ag}$  (2.8741(7) Å) and  $\text{Hg2}\cdots\text{Ag}$  (2.9472(7) Å) distances are less than the sum of the van der Waals radii of Ag (1.72) + Hg (1.73–2.05 Å) and close to the sum of Hg–Ag covalent radii (Hg 1.32 Å + Ag 1.45 Å).<sup>28</sup> The observed Hg–Ag distances indicate a strong  $\text{Hg}^{\text{II}}\cdots\text{Ag}^{\text{I}}$   $d^{10}-d^{10}$  metallophilic interaction. The observed  $\text{Hg}\cdots\text{Ag}$  bond distances are less than the nonbonded  $\text{Hg}\cdots\text{Ag}$  distances (3.101(1), 3.386(1) Å) in  $[\text{HgAg}_2(\text{mes})_2(\text{O}_3\text{SCF}_3)_2]_2$ .<sup>19d</sup> They are comparable to Hg–Ag distances of 2.805(2) and 2.85(3) Å observed in  $[\text{AgHg}_2(\mu\text{-dppm})_3](\text{O}_3\text{SCF}_3)_3$ <sup>19c</sup> and similar Hg/Ag clusters.<sup>19f</sup> The C–Hg–C bond angles [ $\angle\text{C1B}-\text{Hg1}-\text{C1A}$   $178.9(3)^\circ$  and  $\angle\text{C16A}-\text{Hg2}-\text{C16B}$   $176.3(3)^\circ$ ] are close to  $180^\circ$ . The packing diagram reveals that out of the four oxygens of the  $\text{ClO}_4^-$ , two oxygens interact with one mercury atom and one of the hydrogens of the macrocycle.

A comparison of the structure of the copper complex (**14**)<sup>22a</sup> (Figure 8) with the structure of the silver complex (**17**) reveals close similarities. The geometry around both the guest metal ions is distorted octahedral. The  $\angle\text{Hg}-\text{Ag}-\text{N}$  angles are in the range  $\sim 63.63-72.99^\circ$  as compared to the  $\angle\text{Hg}-\text{Cu}-\text{N}$  angles,  $\sim 69.69-73.04^\circ$ . Similarly,  $\angle\text{N1A}-\text{Ag}-\text{N2A}$  ( $76.0(2)^\circ$ ),  $\angle\text{N1B}-\text{Ag}-\text{N2B}$  ( $76.1(2)^\circ$ ),  $\angle\text{N1}-\text{Cu}-\text{N2}$  ( $83.81^\circ$ ), and  $\angle\text{N3}-\text{Cu}-\text{N4}$  ( $83.57^\circ$ ) are comparable. However,  $\angle\text{Hg1}-\text{Ag}-\text{Hg2}$  ( $166.50(3)^\circ$ ) is quite different from  $\angle\text{Hg1}-\text{Cu}-\text{Hg2}$  ( $177.88(3)^\circ$ ).

Colorless crystals of **19** were obtained by slow evaporation of a chloroform/hexane solution. It crystallizes in the orthorhombic crystal system, in the *Pnma* space group. The molecule has a 2-fold axis that passes through the ethane bridge, and only half the molecule represents the asymmetric unit with the  $\mu$ -hydroxo group located at the special position. The C8 carbon, which is disordered, is refined by taking two positions with 0.5 occupancy for each. The molecular structure confirmed cleavage of the macrocycle and formation of a cationic bis(Lewis acid), which traps a hydroxo group. Cleavage of the macrocycle in the case of **19** might be due to the larger size and higher charge on mercury(II). There are no reports in the literature on the complexation of dicationic metal ions with metallamacrocycles/metallacryptands containing dicationic metal ions through a metallophilic interaction. It is worth noting that Catalano and co-workers were unable to synthesize a metallocryptand with a  $\text{Au}(1^+)-\text{Pb}(2^+)$  interaction.<sup>20b</sup> They were able to isolate only systems with  $(1^+)-(0)$  and  $(2^+)-(0)$  charged metallophilic interactions. In addition to the cleavage of the mercury–carbon bond, the other important aspect of this structure is trapping of the hydroxo group between two Lewis acidic mercury centers. There are very few reports of such complexes that incorporate a hydroxo group between two Hg(II) ions.<sup>33,34</sup>

The geometry about each mercury atom is T-shaped, having bonds with carbon, nitrogen, and oxygen (Figure 9). The Hg–N distances are 2.669(8) Å. Hg1–O1 bond distance of 2.069(6) Å is less than the Hg–O bond distance observed in the tetradentate Lewis acid (2.08(1) Å) reported by Wuest

and co-workers.<sup>8c</sup> However, this distance is longer than the Hg–O distance in the hydrated  $[(\text{PhHg})_2\text{OH}]^+$  cation.<sup>34</sup> The observed distance is close to the sum of covalent radii (Hg 1.32 Å + O 0.66 Å = 1.98 Å). The geometry around the oxygen atom in **19** is bent, with the Hg1–O–Hg1 bond angle being  $109.3(4)^\circ$ . This value is larger than the Hg–O–Hg value reported for  $[(\text{PhHg})_2\text{OH}]^+$  ( $126^\circ$ ), but is smaller than the value of  $119.8(4)^\circ$  reported for  $[(1,7\text{-C}_{10}\text{H}_{10})_2\text{Hg}_4(\text{OH})_2][\text{CF}_3\text{CO}_2]_2$ .<sup>33b</sup> Two fluoro groups of the anion are involved in hydrogen bonding with the hydrogen of the  $\mu$ -hydroxo group with an  $\text{F}2\cdots\text{H}$  distance of 2.388 Å. The Hg1–Hg1 distance (3.3753(7) Å) in **19**, though less than the sum of van der Waals radii (3.46–4.1 Å;  $r_{\text{vwd}}$  Hg = 1.73–2.05 Å), may not be a case of  $d^{10}-d^{10}$  interaction. The close distance between the two mercury atoms may be a consequence of geometrical constraint.

In the reactions of macrocycles **6** and **7** with  $\text{Pd}^{\text{II}}$ , a facile transmetalation of the aryl group from mercury to palladium takes precedence over coordination by nitrogen/mercury and results in the formation of **20** and **9**, respectively, with cis disposition of the aryl groups to the palladium. The crystal structure of the dichloromethane solvate of **9** showed a unique  $\text{Hg}^{\text{II}}\cdots\text{Pd}^{\text{II}}\cdots\text{Hg}^{\text{II}}$  interaction.<sup>22b</sup> Crystallization of **9** from acetone gave the pseudopolymorph **9a** in small amount that contains four molecules of **8** in an asymmetric unit and acetone as solvent of crystallization. Compounds **9** and **9a** have low solubility in common organic solvents such as acetone, dichloromethane, and DMSO. The  $\text{Hg}\cdots\text{Pd}$  distances in the asymmetric unit of **9a** are Hg1A $\cdots$ Pd1A 3.1054(9), Hg2A $\cdots$ Pd1A 3.2181(10), Hg1B $\cdots$ Pd1B 3.1524(9), Hg2B $\cdots$ Pd1B 3.1896(10), Hg1C $\cdots$ Pd1C 3.1496(9), Hg2C $\cdots$ Pd1C 3.2201(9), Hg1D $\cdots$ Pd1D 3.1092(9), and Hg2D $\cdots$ Pd1D 3.2150(10) Å. The corresponding distances in the dichloromethane solvate were 3.1020(3) Å (Hg1 $\cdots$ Pd) and 3.2337(3) Å (Hg2 $\cdots$ Pd), which are close to those observed by Gabbai and co-workers in the  $\text{Pd}^{\text{II}}\cdots\text{Hg}^{\text{II}}\cdots\text{Pd}^{\text{II}}$  intermolecular system.<sup>17</sup> The  $\text{Hg}\cdots\text{Pd}$  distances in **9a** as well as **9** are not identical within the same molecule, and the difference between the two  $\text{Hg}\cdots\text{Pd}$  distances in **9a** is 0.1127 Å. The helical nature of the molecule may be responsible for the difference in the two  $\text{Hg}\cdots\text{Pd}$  distances. The  $\text{Hg}^{\text{II}}\cdots\text{Pd}^{\text{II}}\cdots\text{Hg}^{\text{II}}$  angles in the acetone solvate are  $\angle\text{Hg1A}\cdots\text{Pd1A}\cdots\text{Hg2A}$   $164.98(3)^\circ$ ,  $\angle\text{Hg1B}\cdots\text{Pd1B}\cdots\text{Hg2B}$   $161.22(3)^\circ$ ,  $\angle\text{Hg1C}\cdots\text{Pd1C}\cdots\text{Hg2C}$   $162.22(3)^\circ$ , and  $\angle\text{Hg1D}\cdots\text{Pd1D}\cdots\text{Hg2D}$   $165.10(3)^\circ$  as compared to  $162.898(7)^\circ$  observed in the dichloromethane solvate. Complex **9a** has a metallohelicate structure along the  $\text{Hg}^{\text{II}}\cdots\text{Pd}^{\text{II}}\cdots\text{Hg}^{\text{II}}$  axis and is deviated from linearity due to secondary  $\text{N}\cdots\text{Hg}$  interactions.

A closer look at the crystal structure of **9a** reveals that two molecules in the asymmetric unit are linked by an intermolecular  $\text{Hg}\cdots\pi$  interaction (3.773 Å) (Figure 11)

## Conclusion

Using the approach of intramolecular coordination, we have achieved a convenient template-free synthesis of mercurazametallamacrocycles in good yield. The 22-membered macrocycles have a twisted conformation (“hour glass” or figure 8). These macrocycles easily trap  $\text{Cu}^{\text{I}}$  and  $\text{Ag}^{\text{I}}$  ions and exhibit strong  $\text{Hg}^{\text{II}}\cdots\text{Cu}^{\text{I}}\cdots\text{Hg}^{\text{II}}$  and  $\text{Hg}^{\text{II}}\cdots\text{Ag}^{\text{I}}\cdots\text{Hg}^{\text{II}}$  metallophilic interactions. With  $\text{Pd}^{\text{II}}$  and  $\text{Pt}^{\text{II}}$ , transmetalation leads to cleavage of the macrocycles. We have also succeeded in isolating an 11-membered mercurazamacrocycle

(32) (a) Burini, A.; Fackler, J. P., Jr.; Galassi, R.; Pietroni, B. R.; Staples, R. J. *Chem. Commun.* **1998**, 95–96. (b) Silong, S. B.; Kildea, J. D.; White, A. H. *Aust. J. Chem.* **1989**, 42, 1387–1391.

(33) (a) Grdenić, D.; Matković-Calogović, D.; Sikirica, M. *J. Organomet. Chem.* **1987**, 319, 1–8. (b) Zheng, Z.; Knobler, C. B.; Curtis, C. E.; Hawthorne, M. F. *Inorg. Chem.* **1995**, 34, 432–435.

(34) Nicholson, B. K.; Whitton, A. J. *J. Organomet. Chem.* **1986**, 306, 139–144.

in which the  $\angle\text{C}-\text{Hg}-\text{C}$  angle is  $\sim 135^\circ$  and is most deviated from linearity compared to any diorganomercury compound. Interestingly, attempted coordination of  $\text{Hg}^{\text{II}}$  with **6** leads to facile cleavage of the ring and entrapment of a hydroxide ion. This entrapment is facilitated by inadvertent formation of a cationic, chelating bis(Lewis acid) based on an organomercury derivative.

## Experimental Section

**General Experimental Procedures.** All reactions were carried out under nitrogen or argon using standard vacuum-line techniques. The solvents were purified by standard procedures and were freshly distilled prior to use.  $\text{Cu}(\text{CH}_3\text{CN})_4\text{ClO}_4$  was prepared by a reported procedure.<sup>35</sup> Synthesis of compounds **6**, **7**, **10**, and **11** has been earlier described in the literature.<sup>22</sup>  $\text{AgClO}_4$  and *trans*-1,2-diaminocyclohexane were purchased from Aldrich. All the other reagents and solvents used for the reactions were of reagent grade.

**Caution:** The reactions involving mercury compounds were carried out in a well-ventilated fume hood with proper precautions due to their hazardous nature.

**Instrumentation.** Melting points were recorded in capillary tubes. Elemental analyses were performed on a Carlo-Erba model 1106 elemental analyzer. IR spectra were recorded as KBr pellets on a Nicolet Impact 400 and Perkin FT-IR spectrometer. All UV-vis spectra were recorded on a Jasco-570 spectrophotometer. Emission spectra were recorded by using a Perkin-Elmer LS55 luminescence spectrometer.  $^1\text{H}$  (300.4 and 400.5 MHz) and  $^{13}\text{C}$  (100.5 MHz, 75.4 MHz) NMR spectra were recorded on a Varian VXR 300S and a Varian 400 MHz spectrometer, and the  $^{199}\text{Hg}$  ( $^{199}\text{Hg}$ , 53.7 MHz) NMR spectra were recorded on a Bruker DPX300-NMR spectrometer at the indicated frequencies.  $^{19}\text{F}$  (470.3 MHz) NMR was recorded on a Varian 500 MHz spectrometer with  $\text{C}_6\text{F}_6$  as external standard. Chemical shifts cited were referenced to TMS ( $^1\text{H}$ ,  $^{13}\text{C}$ ) as internal and  $\text{Ph}_2\text{Hg}$  ( $^{199}\text{Hg}$ ) as external standard. The electron spray mass spectra (ESI-MS) were performed on a Q-ToF micro (YA-105) mass spectrometer. Mass spectra were obtained with a Platform II single quadrupole mass spectrometer (Micromass, Altrincham, UK) using a  $\text{CH}_3\text{OH}$  mobile phase. Cyclic voltammetric measurements were carried out using a PAR model 273A electrochemistry system. A platinum wire working electrode, a platinum wire auxiliary electrode, and saturated calomel reference electrode were used in a standard three-electrode configuration. Tetraethylammonium perchlorate was the supporting electrolyte, the scan rate used was  $50\text{ mV s}^{-1}$ , and ferrocene was used as standard. All of the electrochemical experiments were carried out under a nitrogen atmosphere, and all of the redox potentials are uncorrected for junction potentials.

**Synthesis of Compound 12.** A solution of **11** (0.41 g, 0.99 mmol) in methanol (100 mL) was added dropwise to a stirred solution of *trans*-1,2-diaminocyclohexane (0.11 g, 0.96 mmol) in methanol (200 mL) over a period of 5–6 h. The mixture was stirred overnight, and the precipitated white powder was filtered off. The filtrate was evaporated under reduced pressure, and the residue obtained was washed with methanol 2–3 times. It was recrystallized from a chloroform and hexane mixture to give square-shaped white crystals of **12**. Yield: 0.33 g (0.34 mmol, 68%), mp  $280\text{--}282^\circ\text{C}$ .  $^1\text{H}$  NMR (400 MHz,  $\text{CDCl}_3$ ):  $\delta$  7.54 (d, 4H,  $J = 9.2\text{ Hz}$ ), 7.42 (t, 4H,  $J = 9.40\text{ Hz}$ ), 7.26 (t, 4H,  $J = 9.60\text{ Hz}$ ), 7.05 (s, 4H), 6.96 (d, 4H,  $J = 9.60\text{ Hz}$ ), 3.0 (s, 4H), 1.25–1.65 (m, 16H).  $^{13}\text{C}$  NMR (100.05 MHz,  $\text{CDCl}_3$  with 2 drops of  $d_6$ -DMSO):  $\delta$  166.8, 166.6, 144.2, 137.9, 132.8, 130.4, 126, 71.7, 35.2, 25.0.  $^{199}\text{Hg}$  NMR (53.05 MHz,  $\text{CDCl}_3$ ):  $\delta$  -667 ppm. IR (KBr):  $1632\text{ }\nu(\text{C}=\text{N})$ ,  $1561$ ,  $1446\text{ cm}^{-1}$ . ESI-MS:  $m/z$

(%) 979 (100)  $[\text{M}]^+$ , 491 (60). UV/vis ( $\text{CHCl}_3$ ;  $\lambda_{\text{max}}$  ( $\epsilon$ ): 270 (14 000), 294 nm ( $8400\text{ M}^{-1}\text{cm}^{-1}$ ). UV/vis (solid,  $\lambda_{\text{max}}$ ): 330 nm. Emission (solid,  $\lambda_{\text{ex}}$  330 nm):  $\lambda_{\text{max}}$  422, 460, 485, 530 nm. Anal. Calcd for  $\text{C}_{40}\text{H}_{40}\text{Hg}_2\text{N}_4$ : C, 49.13; H, 4.12; N, 5.73. Found: C, 49.12; H, 4.12; N, 5.67.

**Synthesis of Compound 13.** Schiff base macrocycle **6** (0.435 g, 0.500 mmol) was taken in 50 mL of dry methanol. An excess of sodium borohydride was slowly added over a period of 2 h at  $0^\circ\text{C}$ . The reaction mixture was stirred at room temperature for 5 h. After refluxing it for 2 h, the solvent was evaporated under vacuum. The residue was quenched with water to destroy the unreacted sodium borohydride and then extracted with dichloromethane ( $3 \times 15\text{ mL}$ ) and dried over sodium sulfate. The workup afforded the crude compound, which was recrystallized from dichloromethane and petroleum ether. Yield: 0.052 g (0.12 mmol, 11%), mp  $166\text{--}168^\circ\text{C}$ .  $^1\text{H}$  NMR (300 MHz,  $\text{CDCl}_3$ ):  $\delta$  7.58 (d, 2H,  $J = 7.32\text{ Hz}$ ), 7.26 (m, 4H) 7.15 (t, 2H,  $J = 7.32\text{ Hz}$ ), 3.89 (s, 4H), 2.80 (s, 4H).  $^{13}\text{C}$  NMR (75.42 MHz,  $\text{CDCl}_3$ ):  $\delta$  168.2, 148.2, 139.1, 128.1, 126.9, 126.4, 48.3, 55.0.  $^{199}\text{Hg}$  NMR (53.05 MHz,  $\text{CDCl}_3$ ):  $\delta$  -572 ppm. IR (KBr):  $3312\text{ }\nu(\text{N}-\text{H})\text{ cm}^{-1}$ . ESI-MS:  $m/z$  (%) 441.8 (55)  $[\text{M} + 2]^+$ . Anal. Calcd for  $\text{C}_{16}\text{H}_{16}\text{HgN}_2$ : C, 43.99; H, 3.69; N, 6.41. Found: C, 43.57; H, 3.93; N, 6.03.

**Synthesis of Compound 16.** To a two-necked round-bottomed flask containing Schiff base **12** (0.195 g, 0.199 mmol) in dry methanol (30 mL) was added  $[\text{Cu}(\text{CH}_3\text{CN})_4]\text{ClO}_4$  (0.065 g, 0.199 mmol). The color of the suspension changed to red immediately. On stirring the reaction mixture for 4 h, a red-colored precipitate was obtained. The precipitate was filtered, washed with methanol, and dried to obtain **16**. The orange-colored filtrate was concentrated, and further slow evaporation gave **16** as a red, crystalline solid. Yield: 0.18 g (0.16 mmol, 79%).  $^1\text{H}$  NMR (400 MHz,  $\text{CDCl}_3$ ):  $\delta$  8.10 (s, 4H), 7.56 (m, 8H), 7.46 (t, 4H,  $J = 9.20\text{ Hz}$ ), 7.30 (d, 4H,  $J = 10.4\text{ Hz}$ ), 2.80 (s, br, 4H), 2.02 (s, br, 4H), 1.75 (s, br, 4H), 1.19 (s, 8H).  $^{13}\text{C}$  NMR (100.05 MHz,  $\text{CDCl}_3$ ):  $\delta$  169.1, 166.8, 143.8, 137.9, 132.6, 132.6, 128.1, 68.5, 32.1, 24.2.  $^{199}\text{Hg}$  NMR (53.05 MHz,  $\text{CDCl}_3$ ):  $\delta$  -495 ppm. IR (KBr):  $1627\text{ }\nu(\text{C}=\text{N})$ ,  $1092$ ,  $626\text{ }\nu(\text{ClO}_4^-)\text{ cm}^{-1}$ . ESI-MS:  $m/z$  (%) 1041 (100)  $[\text{M} - \text{ClO}_4]^+$ . UV/vis ( $\text{CHCl}_3$ ;  $\lambda_{\text{max}}$  ( $\epsilon$ ): 269 (10 000), 294 (7800), 421 nm ( $960\text{ M}^{-1}\text{cm}^{-1}$ ). UV/vis (solid,  $\lambda_{\text{max}}$ ): 340, 475 nm. Emission (solid,  $\lambda_{\text{ex}}$  475 nm):  $\lambda_{\text{max}}$  530 nm. Anal. Calcd for  $\text{C}_{40}\text{H}_{40}\text{ClCuHg}_2\text{N}_4\text{O}_4$ : C, 42.11; H, 3.53; N, 4.91. Found: C, 41.93; H, 3.43; N, 4.87.

**Synthesis of Compound 17.** A similar reaction of Schiff base ligand **6** (0.219 g, 0.252 mmol) with silver perchlorate (0.052 g, 0.252 mmol) in methanol (20 mL) afforded a white precipitate of complex **17**. Yield: 0.17 g (0.16 mmol, 63%).  $^1\text{H}$  NMR (400 Hz,  $\text{CD}_3\text{CN}$ ):  $\delta$  8.28 (s, 4H), 7.55 (m, 8H), 7.32 (m, 4H), 7.17 (d, 4H), 3.64 (s, 8H).  $^{13}\text{C}$  NMR (75.42 MHz,  $\text{CD}_3\text{CN}$ ):  $\delta$  172.5, 144.7, 139.1, 133.1, 132.5, 128.3, 165.8, 66.7.  $^{199}\text{Hg}$  NMR (53.05 MHz,  $\text{CDCl}_3$ ):  $\delta$  -552 ppm. IR (KBr):  $1627\text{ }\nu(\text{C}=\text{N})\text{ cm}^{-1}$ . ESI-MS:  $m/z$  (%) 977 (30)  $[\text{M} - \text{ClO}_4]^+$ . UV/vis ( $\text{CH}_3\text{CN}$ ,  $\lambda_{\text{max}}$  ( $\epsilon$ ): 270 (14 000), 294 nm ( $9400\text{ M}^{-1}\text{cm}^{-1}$ ). Emission (solid,  $\lambda_{\text{ex}}$  336 nm):  $\lambda_{\text{max}}$  422, 460, 485, 530 nm. Anal. Calcd for  $\text{C}_{32}\text{H}_{28}\text{AgClHg}_2\text{N}_4\text{O}_4$ : C, 35.68; H, 2.62; N, 5.20. Found: C, 34.62; H, 2.75; N, 5.29.

**Synthesis of Compound 18.** To a two-necked round-bottomed flask with 30 mL of degassed methanol was added ligand **6** (0.219 g, 0.252 mmol). After some time  $\text{AgNO}_3$  (0.042 g, 0.252 mmol) was added and the reaction mixture stirred at room temperature overnight. To the reaction mixture was added an excess of ammonium hexafluorophosphate. The resulting white precipitate was filtered off, and the filtrate was kept for crystallization. After evaporation of the solvent, a pale white precipitate of **18** was obtained. Yield: 0.16 g (0.14 mmol, 57%), mp  $210\text{--}212^\circ\text{C}$ .  $^1\text{H}$  NMR (400 MHz,  $\text{CD}_3\text{CN}$ ):  $\delta$  8.36 (s, 4H), 7.56 (d, 8H,  $J = 5.2$ ), 7.34 (m, 4H), 7.17 (d, 4H,  $J = 9.60$ ), 3.71 (s, 8H).  $^{13}\text{C}$  NMR (100.05 MHz,  $\text{CD}_3\text{CN}$ ):  $\delta$  172.5, 168.8, 144.7, 139.1, 133.1, 132.5, 128.4, 60.7.  $^{199}\text{Hg}$  NMR (53.05 MHz,  $\text{CDCl}_3$ ):  $\delta$  -555 ppm. IR (KBr):  $1627\text{ }\nu(\text{C}=\text{N})\text{ cm}^{-1}$ . ESI-MS:

(35) Simmons, M. G.; Merrill, C. L.; Wilson, L. J.; Bottomley, L. A.; Kadish, K. M. *J. Chem. Soc., Dalton Trans.* **1980**, 1827–1837.

Table 2. Crystallographic Data of 6, 7, 10, and 12

	6	7	10	12
empirical formula	C <sub>32</sub> H <sub>28</sub> Hg <sub>2</sub> N <sub>4</sub>	C <sub>40</sub> H <sub>28</sub> Hg <sub>2</sub> N <sub>4</sub>	C <sub>14</sub> H <sub>14</sub> HgO <sub>2</sub>	C <sub>40</sub> H <sub>40</sub> Hg <sub>2</sub> N <sub>4</sub>
fw	869.76	965.84	414.84	977.94
cryst syst	monoclinic	monoclinic	monoclinic	orthorhombic
space group	<i>Pc</i>	<i>P2<sub>1</sub>/c</i>	<i>P2<sub>1</sub>/n</i>	<i>Pcan</i>
<i>a</i> (Å)	9.3680(19)	18.3577(16)	4.9461(5)	12.8247(8)
<i>b</i> (Å)	9.2432(19)	8.6721(8)	18.807(2)	15.5549(9)
<i>c</i> (Å)	16..261(3)	41.832(4)	12.9982(15)	17.1838(10)
α (deg)	90	90	90	90
β (deg)	91.123(4)	100.7450(10)	94.976(2)	90
γ (deg)	90	90	90	90
<i>V</i> (Å <sup>3</sup> )	1407.8(5)	6542.9(10)	1204.5(2)	3427.9(4)
<i>Z</i>	2	8	4	4
<i>d</i> (calcd) (Mg/m <sup>3</sup> )	2.052	1.961	2.288	1.895
temp (K)	293(2)	293(2)	103(2)	103(2)
λ (Å)	0.71073	0.71073	0.71073	0.71073
range of θ (deg)	2.17 to 28.30	2.09 to 30.93	1.91 to 28.31	2.38 to 28.29
abs coeff (mm <sup>-1</sup> )	10.920	9.409	12.763	8.981
obsd reflens [ <i>I</i> > 2σ]	10 499	19 140	9182	25 199
final <i>R</i> ( <i>F</i> ) [ <i>I</i> > 2σ( <i>I</i> )]	0.0679	0.0415	0.0203	0.0222
<i>wR</i> ( <i>F</i> <sup>2</sup> ) indices [ <i>I</i> > 2σ]	0.1753	0.0924	0.0498	0.0517
data/restraints/params	4801/182/296	19 140/0/ 829	2905/0/154	4177/0/209
goodness of fit on <i>F</i> <sup>2</sup>	1.106	1.010	1.063	0.953

Table 3. Crystallographic Data of 13, 17, 19, and 9a

	13	17	19	9a(acetone solvate)
empirical formula	C <sub>16</sub> H <sub>18</sub> HgN <sub>2</sub>	C <sub>32</sub> H <sub>28</sub> AgClHg <sub>2</sub> N <sub>4</sub> O <sub>4</sub>	C <sub>16</sub> H <sub>15</sub> F <sub>6</sub> Hg <sub>2</sub> N <sub>2</sub> OP	C <sub>83</sub> H <sub>62</sub> Cl <sub>4</sub> Hg <sub>4</sub> N <sub>8</sub> OPd <sub>2</sub>
fw	438.91	1077.08	797.45	2344.37
cryst syst	orthorhombic	monoclinic	orthorhombic	monoclinic
space group	<i>Cmc2<sub>1</sub></i>	<i>P2<sub>1</sub>/c</i>	<i>Pnma</i>	<i>C2/c</i>
<i>a</i> (Å)	21.7105(18)	14.9546(16)	8.7266(5)	41.2863(7)
<i>b</i> (Å)	7.1769(8)	10.5319(11)	17.9057(11)	19.3267(2)
<i>c</i> (Å)	8.9718(8)	19.534(2)	12.5696(8)	41.0150(7)
α (deg)	90	90	90	90
β (deg)	90	90.001(2)	90	109.957(2)
γ (deg)	90	90	90	90
<i>V</i> (Å <sup>3</sup> )	1397.9(2)	3076.5(6)	1964.1(2)	30761.7(8)
<i>Z</i>	4	4	4	16
<i>d</i> (calcd) (Mg/m <sup>3</sup> )	2.085	2.325	2.697	2.025
temp (K)	193(2)	100(2)	293(2)	200(2)
λ (Å)	0.71073	0.71073	0.71073	1.54184
range of θ (deg)	2.99 to 26.69	1.36 to 28.27	3.06 to 26.73	4.10 to 73.78
abs coeff (mm <sup>-1</sup> )	10.998	10.718	15.764	19.336
obsd reflens [ <i>I</i> > 2σ]	7261	23 361	2148	29 988
final <i>R</i> ( <i>F</i> ) [ <i>I</i> > 2σ( <i>I</i> )]	0.0245	0.0428	0.0297	0.0488
<i>wR</i> ( <i>F</i> <sup>2</sup> ) indices [ <i>I</i> > 2σ]	0.0584	0.1035	0.0651	0.1202
data/restraints/params	1517/2/92	7461/0/397	2148/41/144	29 888/0/ 1841
goodness of fit on <i>F</i> <sup>2</sup>	1.092	1.029	0.947	0.934

*m/z* (%) 977 (18) [M – PF<sub>6</sub>]<sup>+</sup>, 565 (10) [1/2 M<sup>+</sup>]. UV/vis (CH<sub>3</sub>CN, λ<sub>max</sub> (ε)): 270 (14 000), 294 nm (9500 M<sup>-1</sup>cm<sup>-1</sup>). Emission (solid, λ<sub>ex</sub> 336 nm): λ<sub>max</sub> 422, 460, 485, 530 nm. Anal. Calcd for C<sub>32</sub>H<sub>28</sub>AgF<sub>6</sub>Hg<sub>2</sub>N<sub>4</sub>P: C, 34.24; H, 2.51; N, 4.99. Found: C, 33.98; H, 2.60; N, 4.89.

**Synthesis of Compound 19.** To a solution of **6** (0.219 g, 0.252 mmol) in methanol (25 mL) was added Hg(OCOCH<sub>3</sub>)<sub>2</sub> (0.080 g, 0.252 mmol) in dichloromethane (10 mL) and the reaction mixture stirred for 3 days. After that, an excess of NH<sub>4</sub>PF<sub>6</sub> was added to give a white precipitate, which was crystallized from acetonitrile. Yield: 0.083 g (0.10 mmol, 42%). <sup>1</sup>H NMR (400 MHz, *d*<sub>6</sub>-DMSO): δ 8.74 (s, 2H), 7.65 (d, 2H, *J* = 7.6), 7.56 (m, 4H), 7.44 (t, 2H, *J* = 7.6) 3.9 (s, 4H). <sup>13</sup>C NMR (100.05 MHz, *d*<sub>6</sub>-DMSO): δ 166.2, 148.1, 140.6, 137.9, 133.0, 132.2, 128.6, 61.1. <sup>19</sup>F NMR (470 MHz, *d*<sub>6</sub>-DMSO): δ -67.9 (d, 6F, *J*(<sup>31</sup>P–<sup>19</sup>F) = 711 Hz). <sup>199</sup>Hg NMR (53.05 MHz, *d*<sub>6</sub>-DMSO): δ -1013 ppm. IR (KBr): 1622 ν(C=N) cm<sup>-1</sup>. ESI-MS: *m/z* (%) 651 (100) [M – PF<sub>6</sub>]<sup>+</sup>, 1285 (10). Anal. Calcd for C<sub>16</sub>H<sub>15</sub>-F<sub>6</sub>Hg<sub>2</sub>N<sub>2</sub>OP: C, 24.10; H, 1.90; N, 3.51. Found: C, 23.85; H, 1.63; N, 3.79.

**Synthesis of Compound 20.** To a chloroform (10 mL) solution of **6** (0.219 g, 0.252 mmol) was added dropwise a solution of

Pd(C<sub>6</sub>H<sub>5</sub>CN)<sub>2</sub>Cl<sub>2</sub> (0.096 g, 0.252 mmol) in chloroform. After stirring for 2 h, the reaction mixture was filtered and kept at 0 °C to afford a precipitate of the complex **20**. Yield: 0.14 g (0.13 mmol, 54%), mp 225 °C (dec). IR (KBr): 1640, 1618 cm<sup>-1</sup> ν(C=N). ESI-MS: *m/z* (%) 1011 (45) [M – Cl]<sup>+</sup>. <sup>199</sup>Hg NMR (53.05 MHz, *d*<sub>6</sub>-DMSO): δ -1045 ppm. Anal. Calcd for C<sub>32</sub>H<sub>28</sub>Cl<sub>2</sub>Hg<sub>2</sub>N<sub>4</sub>Pd: C, 36.72; H, 2.69; N 5.34. Found: C, 36.57; H, 2.28; N, 6.27.

**Synthesis of Compound 21.** To a solution of **6** (0.219 g, 0.252 mmol) in chloroform was added dropwise, a solution of Pt-(COD)Cl<sub>2</sub> (0.102 g, 0.273 mmol) in chloroform. It was stirred for 4 h, and the precipitate formed was filtered and washed with acetonitrile several times. The yellow powder formed was characterized as **21**. Yield: 0.17 g (0.15 mmol, 60%), mp 230 °C (dec). IR (KBr): 1642 cm<sup>-1</sup> (br) ν(C=N). ESI-MS: *m/z* (%) 1100 (30) [M – Cl]<sup>+</sup>. <sup>199</sup>Hg NMR (53.05 MHz, *d*<sub>6</sub>-DMSO): δ -1043 ppm. Anal. Calcd for C<sub>32</sub>H<sub>28</sub>Cl<sub>2</sub>Hg<sub>2</sub>N<sub>4</sub>Pt: C, 33.84; H, 2.48; N, 4.93. Found: C, 34.55; H, 2.29; N, 5.06.

**Synthesis of Compound 9a.** To a solution of macrocycle **7** (0.201 g, 0.208 mmol) in dichloromethane (25 mL) was added Pd(C<sub>6</sub>H<sub>5</sub>CN)<sub>2</sub>Cl<sub>2</sub> (0.080 g, 0.208 mmol), and the reaction mixture was stirred for 5 h at room temperature. The yellow

precipitate obtained was filtered, and the filtrate was kept at room temperature for slow evaporation to obtain orange-colored crystals of **9** (0.052 mmol, 0.060 g, 60%). On crystallization of 50 mg of yellow precipitate in acetone, **9a** was obtained in small amount (0.008 g), mp 220–222 °C. IR (KBr): 1617, 1598  $\text{cm}^{-1}$   $\nu(\text{C}=\text{N})$ . Anal. Calcd for  $\text{C}_{83}\text{H}_{62}\text{Cl}_4\text{Hg}_4\text{N}_8\text{OPd}_2$ : C, 42.52; H, 2.67; N, 4.78. Found: C, 43.02; H, 2.46; N, 5.06.

**X-ray Crystallography.** The diffraction measurements for compounds **6**, **7**, **10**, **11**, **12**, **14**,<sup>22a</sup> and **17** were performed on a Bruker P4 and Bruker SMART 1000 CCD and for **13** and **19** on a Stoe IPDS with graphite-monochromated Mo  $\text{K}\alpha$  radiation ( $\lambda = 0.7107 \text{ \AA}$ ). The crystal data for **9a** were collected on a Oxford Diffraction X-Calibur diffractometer using Cu radiation

( $\lambda = 1.5418 \text{ \AA}$ ). The structures were solved by direct methods and full matrix least-squares refinement on  $F^2$  (program SHELXL-97).<sup>36a,b</sup> Hydrogen atoms were localized by geometrical means. A riding model was chosen for refinement. The isotropic thermal parameters of the H atoms were fixed at 1.5 times ( $\text{CH}_3$  groups) or 1.2 times  $U(\text{eq})$  (Ar–H) of the corresponding C atom. The crystals of **6** were invariably found to be pseudomerohedrally twinned. It was solved in  $Pc$  with SIR92.<sup>36c</sup> The twin law was obtained using ROTAX (1 0 0 0 –1 0 0 0 –1).

**Acknowledgment.** H.B.S. is grateful to the Department of Science and Technology (DST), New Delhi, for funding and S.S. thanks UGC for SRF.

(36) (a) Sheldrick, G. M. *SHELXS-97, Program for Crystal Structures Solution*; University of Göttingen: Göttingen, Germany, 1997. (b) Sheldrick, G. M. *SHELXL-97, Program for Crystal Structures Refinement*; University of Göttingen: Göttingen, Germany, 1997. (c) Altomare, A.; Cascarano, G.; Giacovazzo, C.; Guagliardi, A.; Burla, M. C.; Polidori, G.; Camalli, M. *J. Appl. Crystallogr.* **1994**, 27, 435–436.

**Supporting Information Available:** Spectral data ( $^1\text{H}$ ,  $^{13}\text{C}$ ,  $^{199}\text{Hg}$  NMR, emission spectra, and ES-MS) for **13**, **16**, **18**, and **19**; CV of **17**; X-ray crystallographic data of **6**, **7**, **10**, **11**, **12**, **13**, **17**, **19**, and **9a** in CIF format. This material is available free of charge via the Internet at <http://pubs.acs.org>.